

1 **Climate Sensitivity Estimated From Temperature Reconstructions**
2 **of the Last Glacial Maximum**

3

4 Andreas Schmittner,^{1*} Nathan M. Urban,² Jeremy D. Shakun,³ Natalie M. Mahowald,⁴ Peter U.
5 Clark,⁵ Patrick J. Bartlein,⁶ Alan C. Mix,¹ Antoni Rosell-Melé⁷

6 ¹College of Oceanic and Atmospheric Sciences, Oregon State University, Corvallis, OR 97331-
7 5503, USA.

8 ²Woodrow Wilson School of Public and International Affairs, Princeton University, NJ 08544,
9 USA.

10 ³Department of Earth and Planetary Sciences, Harvard University, Cambridge, MA 02138, USA.

11 ⁴Department of Earth and Atmospheric Sciences, Cornell University, Ithaca, NY 14850, USA.

12 ⁵Department of Geosciences, Oregon State University, Corvallis, OR 97331, USA.

13 ⁶Department of Geography, University of Oregon, Eugene, OR 97403, USA.

14 ⁷ICREA and Institute of Environmental Science and Technology, Universitat Autònoma de
15 Barcelona, Bellaterra, Spain.

16

17

18

19 *To whom correspondence should be addressed. E-mail: aschmitt@coas.oregonstate.edu.

20

21

22 *Assessing impacts of future anthropogenic carbon emissions is currently impeded by*
23 *uncertainties in our knowledge of equilibrium climate sensitivity to atmospheric carbon*
24 *dioxide doubling. Previous studies suggest 3 K as best estimate, 2–4.5 K as the 66% probability*
25 *range, and non-zero probabilities for much higher values, the latter implying a small but*
26 *significant chance of high-impact climate changes that would be difficult to avoid. Here,*
27 *combining extensive sea and land surface temperature reconstructions from the Last Glacial*
28 *Maximum with climate model simulations we estimate a lower median (2.3 K) and reduced*
29 *uncertainty (1.7–2.6 K 66% probability). Assuming paleoclimatic constraints apply to the*
30 *future as predicted by our model, these results imply lower probability of imminent extreme*
31 *climatic change than previously thought.*

32

33 Climate sensitivity is the change in global mean surface air temperature ΔSAT caused by
34 an arbitrary perturbation ΔF (radiative forcing) of Earth's radiative balance at the top of the
35 atmosphere with respect to a given reference state. The equilibrium climate sensitivity for a
36 doubling of atmospheric carbon dioxide (CO_2) concentrations (ECS_{2xCO_2}) from preindustrial times
37 has been established as a well-defined standard measure (1). Moreover, because transient
38 (disequilibrium) climate change and impacts on ecological and social systems typically scale
39 with ECS_{2xCO_2} it is a useful and important diagnostic in climate modeling (1). Initial estimates of
40 $ECS_{2xCO_2} = 3 \pm 1.5$ K suggested a large uncertainty (2), which has not been reduced in the last 32
41 years despite considerable efforts (1-10). On the contrary, many recent studies suggest a small
42 but significant possibility of very high (up to 10 K and higher) values for ECS_{2xCO_2} (3-10) implying
43 extreme climate changes in the near future, which would be difficult to avoid. Efforts to use
44 observations from the last 150 years to constrain the upper end of ECS_{2xCO_2} have met with limited

45 success, largely because of uncertainties associated with aerosol forcing and ocean heat uptake
46 (8, 9). Data from the Last Glacial Maximum (LGM, 19-23,000 years ago) are particularly useful
47 to estimate ECS_{2xC} because large differences from pre-industrial climate and much lower
48 atmospheric CO₂ concentrations (185 ppm versus 280 ppm pre-industrial) provide a favorable
49 signal-to-noise ratio, both radiative forcings and surface temperatures are relatively well
50 constrained from extensive paleoclimate reconstructions and modeling (11-13), and climate
51 during the LGM was close to equilibrium, avoiding uncertainties associated with transient ocean
52 heat uptake.

53 Here we combine a climate model of intermediate complexity with syntheses of
54 temperature reconstructions from the LGM to estimate ECS_{2xC} using a Bayesian statistical
55 approach. LGM, 2×CO₂ and pre-industrial control simulations are integrated for 2000 years
56 using an ensemble of 47 versions of the University of Victoria (UVic) climate model (14) with
57 different climate sensitivities ranging from $ECS_{2xC} = 0.3$ to 8.3 K considering uncertainties in
58 water vapor, lapse rate and cloud feedbacks on the outgoing infrared radiation (Fig. S1), as well
59 as uncertainties in dust forcing and wind stress response. The LGM simulations include larger
60 continental ice sheets, lower greenhouse gas concentrations, higher atmospheric dust levels (Fig.
61 S2) and changes in the seasonal distribution of solar radiation (see SOM). We combine recent
62 syntheses of global sea surface temperatures (SSTs) from the Multiproxy Approach for the
63 Reconstruction of the Glacial Ocean (MARGO) project (12) and surface air temperatures over
64 land based on pollen evidence (13), with additional data from ice sheets, land and ocean
65 temperatures (SOM; all reconstructions include error estimates Fig. S3). The combined dataset
66 covers over 26% of Earth's surface (Fig. 1, top panel).

67 Figure 2 compares reconstructed zonally averaged surface temperatures with model

68 results. Models with $ECS_{2xC} < 1.3$ K underestimate the cooling at the LGM almost everywhere,
69 particularly at mid latitudes and over Antarctica, whereas models with $ECS_{2xC} > 4.5$ K
70 overestimate the cooling almost everywhere, particularly at low latitudes. High sensitivity
71 models ($ECS_{2xC} > 6.3$ K) show a runaway effect resulting in a completely ice-covered planet.
72 Once snow and ice cover reach a critical latitude, the positive ice-albedo feedback is larger than
73 the negative feedback due to reduced longwave radiation (Planck feedback), triggering an
74 irreversible transition (Fig. S4) (15). During the LGM Earth was covered by more ice and snow
75 than it is today, but continental ice sheets did not extend equatorward of $\sim 40^\circ\text{N/S}$, and the tropics
76 and subtropics were ice free except at high altitudes. Our model thus suggests that large climate
77 sensitivities ($ECS_{2xC} > 6$ K) cannot be reconciled with paleoclimatic and geologic evidence, and
78 hence should be assigned near-zero probability.

79 Posterior probability density functions (PDFs) of the climate sensitivity are calculated by
80 Bayesian inference, using the likelihood of the observations ΔT_{obs} given the model
81 $\Delta T_{mod}(ECS_{2xC})$ at the locations of the observations. The two are assumed to be related by an error
82 term ε , $\Delta T_{obs} = \Delta T_{mod}(ECS_{2xC}) + \varepsilon$, which represents errors in both the model (endogenously
83 estimated separately for land and ocean) and the observations (Fig. S3), including spatial
84 autocorrelation. A Gaussian likelihood function and an autocorrelation length scale of $\lambda = 2000$
85 km are assumed. The choice of the autocorrelation length scale is motivated by the model
86 resolution and by residual analysis. (See sections 5 and 6 in the SOM for a full description of the
87 statistical method, assumptions, and sensitivity tests.)

88 The resulting PDF (Fig. 3), considering both land and ocean reconstructions, is multi-
89 modal and displays a broad maximum with a double peak between 2 and 2.6 K, smaller local
90 maxima around 2.8 K and 1.3 K and vanishing probabilities below 1 K and above 3.2 K. The

91 distribution has its mean and median at 2.2 K and 2.3 K, respectively and its 66% and 90%
92 cumulative probability intervals are 1.7–2.6 K, and 1.4–2.8 K, respectively. Using only ocean
93 data the PDF changes little, shifting towards slightly lower values (mean 2.1 K, median 2.2 K,
94 66% 1.5 – 2.5 K, 90% 1.3 – 2.7 K), whereas using only land data leads to a much larger shift
95 towards higher values (mean and median 3.4 K, 60% 2.8 – 4.1 K, 90% 2.2 – 4.6 K).

96 The best-fitting model ($ECS_{2xC} = 2.4$ K) reproduces well the reconstructed global mean
97 cooling of 2.2 K (within two significant digits), as well as much of the meridional pattern of the
98 zonally averaged temperature anomalies (correlation coefficient $r = 0.8$; Fig. 2). Significant
99 discrepancies occur over Antarctica, where the model underestimates the observed cooling by
100 almost 4 K, and between 45-50° in both hemispheres, where the model is also too warm.
101 Simulated temperature changes over Antarctica show considerable spatial variations (Fig. 1),
102 with larger cooling of more than 7 K over the West Antarctic Ice Sheet. The observations are
103 located along a strong meridional gradient (Fig. S7). Zonally averaged cooling of air
104 temperatures is about 7 K at 80°S, more consistent with the reconstructions than the simulated
105 temperature change at the locations of the observations. Underestimated ice sheet height at these
106 locations could be a reason for the bias (16), as could be deficiencies of the simple energy
107 balance atmospheric model component. Underestimated cooling at mid-latitudes for the best
108 fitting model also points to systematic model problems, such as the neglect of wind or cloud
109 changes.

110 Two-dimensional features in the reconstructions are less well reproduced by the model (r
111 $= 0.5$; Fig. 1). Large-scale patterns that are qualitatively captured (Fig. 1) are stronger cooling
112 over land than over the oceans, and more cooling at mid to high latitudes (except for sea ice
113 covered oceans), which is contrasted by less cooling in the central Pacific and over the southern

114 hemisphere subtropical oceans. Continental cooling north of 40°N of 7.7 K predicted by the best-
115 fitting model is consistent with the independent estimate of 8.3 ± 1 K from inverse ice-sheet
116 modeling (17).

117 Generally the model solution is much smoother than the reconstructions partly because of
118 the simple diffusive energy balance atmospheric model component. The model does not simulate
119 warmer surface temperatures anywhere, while the reconstructions show warming in the centers
120 of the subtropical gyres, in parts of the northwest Pacific, Atlantic, and Alaska. It systematically
121 underestimates cooling over land and overestimates cooling of the ocean (Fig. S8). The land-sea
122 contrast, which is governed by less availability of water for evaporative cooling over land
123 compared with the ocean (18), is therefore underestimated, consistent with the tension between
124 the ECS_{2xC} inferred from ocean only versus land only data (Fig. 3). A possible reason for this
125 bias could be overestimated sea-to-land water vapor transport in the LGM model simulations
126 perhaps due to too high moisture diffusivities. Other model simplifications such as neglecting
127 changes in wind velocities and clouds or errors in surface albedo changes in the dynamic
128 vegetation model component could also contribute to the discrepancies. The ratio between land
129 and sea temperature change in the best-fitting model is 1.2, which is lower than the modern ratio
130 of 1.5 found in observations and modeling studies (19).

131 Despite these shortcomings, the best-fitting model is within the 1σ -error interval of the
132 reconstructed temperature change in three quarters (75%, mostly over the oceans) of the global
133 surface area covered by reconstructions (Fig. S8). The model provides data constrained estimates
134 of global mean (including grid points not covered by data) cooling of near surface air
135 temperatures $\Delta SAT_{LGM} = -3.0$ K (60% probability range $[-2.1, -3.3]$, 90% $[-1.7, -3.7]$) and sea
136 surface temperatures $\Delta SST_{LGM} = -1.7$ K (60% $[-1.1, -1.8]$, 90% $[-0.9, -2.1]$) during the LGM

137 (including an increase of marine sea and air temperatures of 0.3 K and 0.47 K, respectively, due
138 to 120 m sea-level lowering; otherwise $\Delta SAT_{LGM} = -3.3$ K, $\Delta SST_{LGM} = -2.0$ K).

139 The ranges of 66% and 90% cumulative probability intervals as well as the mean and
140 median ECS_{2xC} values from our study are considerably lower than previous estimates. The most
141 recent assessment report from the Intergovernmental Panel on Climate Change (6), for example,
142 used a most likely value of 3.0 K and a likely range (66% probability) of 2–4.5 K, which was
143 supported by other recent studies (1, 20-23).

144 We propose three possible reasons why our study yields lower estimates of ECS_{2xC} than
145 previous work that also used LGM data. Firstly, the new reconstructions of LGM surface
146 temperatures show less cooling than previous studies. Our best estimates for global mean
147 (including grid points not covered by data) SAT and SST changes reported above are 30–40%
148 smaller than previous estimates (21, 23). This is consistent with less cooling of tropical SSTs (–
149 1.5 K, 30°S–30°N) in the new reconstruction (12) compared with previous datasets (–2.7 K)
150 (24). Tropical Atlantic SSTs between 20°S–20°N are estimated to be only 2.4 K colder during
151 the LGM in the new reconstruction compared to 3 K used in (23), explaining part of the
152 difference between their higher estimates of ECS_{2xC} and ΔSAT_{LGM} (–5.8 K).

153 The second reason is limited spatial data coverage. A sensitivity test excluding data from
154 the North Atlantic leads to more than 0.5 K lower ECS_{2xC} estimates (SOM section 7, Figs. S14,
155 S15). This shows that systematic biases can result from ignoring data outside selected regions as
156 done in previous studies (22, 23) and implies that global data coverage is important for
157 estimating ECS_{2xC} . Averaging over all grid points in our model leads to a higher global mean
158 temperature (SST over ocean, SAT over land) change (–2.6 K) than using only grid points where
159 paleo data are available (–2.2 K), suggesting that the existing dataset is still spatially biased

160 towards low latitudes and/or oceans. Increased spatial coverage of climate reconstructions is
161 therefore necessary in order to improve ECS_{2xC} estimates.

162 A third reason may be the neglect of dust radiative forcing in some previous LGM studies
163 (21) despite ample evidence from the paleoenvironmental record that dust levels were much
164 higher (25, 26). Sensitivity tests (Fig. 3, SOM section 7) show that dust forcing decreases the
165 median ECS_{2xC} by about 0.3 K.

166 Our estimated ECS_{2xC} uncertainty interval is rather narrow, < 1.5 K for the 90%
167 probability range, with most ($\sim 75\%$) of the probability mass between 2 and 3 K, which arises
168 mostly from the SST constraint. This sharpness may imply that LGM SSTs are a strong physical
169 constraint on ECS_{2xC} . However, it could also be attributable to overconfidence arising from
170 physical uncertainties not considered here, or from mis-specification of the statistical model.

171 To explore this, we conduct sensitivity experiments that perturb various physical and
172 statistical assumptions (Figs. 3, S14, S15). The experiments collectively favor sensitivities
173 between 1 and 3 K. However, we cannot exclude the possibility that the analysis is sensitive to
174 uncertainties or statistical assumptions not considered here, and the underestimated land/sea
175 contrast in the model, which leads to the difference between land and ocean based estimates of
176 ECS_{2xC} , remains an important caveat.

177 Our uncertainty analysis is not complete and does not explicitly consider uncertainties in
178 radiative forcing due to ice sheet extent or different vegetation distributions. Our limited model
179 ensemble does not scan the full parameter range, neglecting, for example, possible variations in
180 shortwave radiation due to clouds. Non-linear cloud feedbacks in different complex models
181 make the relation between LGM and $2\times CO_2$ derived climate sensitivity more ambiguous than
182 apparent in our simplified model ensemble (27). More work, in which these and other

183 uncertainties are considered, will be required for a more complete assessment.

184 In summary, using a spatially extensive network of paleoclimate observations in
185 combination with a climate model we find that climate sensitivities larger than 6 K are
186 implausible, and that both the most likely value and the uncertainty range are smaller than
187 previously thought. This demonstrates that paleoclimate data provide efficient constraints to
188 reduce the uncertainty of future climate projections.

189

190 References and Notes

191

192

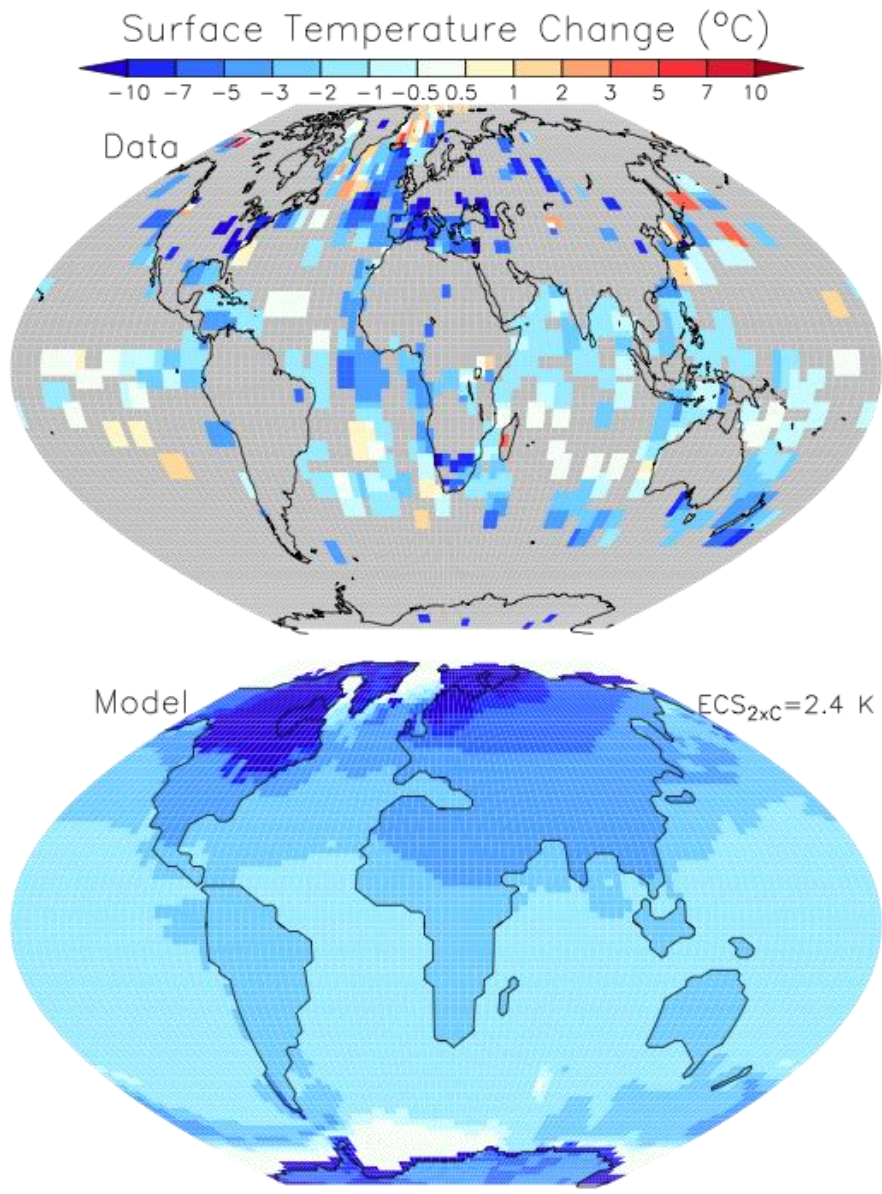
- 193 1. R. Knutti, G. C. Hegerl, *Nat Geosci* **1**, 735 (Nov, 2008).
- 194 2. J. G. Charney *et al.*, “Carbon Dioxide and Climate: A Scientific Assessment” (1979).
- 195 3. D. A. Stainforth *et al.*, *Nature* **433**, 403 (Jan 27, 2005).
- 196 4. G. H. Roe, *Science* **318**, 629 (10.1126/science.1144735, 2007).
- 197 5. D. L. Royer, R. A. Berner, J. Park, *Nature* **446**, 530 (Mar 29, 2007).
- 198 6. IPCC, *Climate Change 2007: The Physical Science Basis. Contribution of Working*
199 *Group I to the Fourth Assessment Report of the Intergovernmental Panel on Climate*
200 *Change*. S. Solomon *et al.*, Eds., (Cambridge University Press, Cambridge, United
201 Kingdom, New York, NY, USA, 2007), pp. 996.
- 202 7. R. Knutti, T. F. Stocker, F. Joos, G. K. Plattner, *Clim Dynam* **21**, 257 (Sep, 2003).
- 203 8. C. E. Forest, P. H. Stone, A. P. Sokolov, *Tellus Series a-Dynamic Meteorology and*
204 *Oceanography* **60**, 911 (Oct, 2008).
- 205 9. N. G. Andronova, M. E. Schlesinger, *Journal of Geophysical Research-Atmospheres* **106**,
206 22605 (Oct 16, 2001).
- 207 10. J. M. Gregory, R. J. Stouffer, S. C. B. Raper, P. A. Stott, N. A. Rayner, *J Climate* **15**,
208 3117 (Nov, 2002).
- 209 11. N. M. Mahowald *et al.*, *Journal of Geophysical Research-Atmospheres* **111**, D10202
210 (May 31, 2006).
- 211 12. MARGO Project Members, *Nat Geosci* **2**, 127 (Feb, 2009).
- 212 13. P. Bartlein *et al.*, *Clim Dynam* **37**, 775 (2011).
- 213 14. A. J. Weaver *et al.*, *Atmos Ocean* **39**, 361 (Dec, 2001).
- 214 15. M. I. Budyko, *Tellus* **21**, 611 (1969).
- 215 16. V. Masson-Delmotte *et al.*, *Clim Dynam* **26**, 513 (Apr, 2006).
- 216 17. R. Bintanja, R. S. W. van de Wal, J. Oerlemans, *Clim Dynam* **24**, 197 (Feb, 2005).
- 217 18. S. Manabe, M. J. Spelman, R. J. Stouffer, *J Climate* **5**, 105 (Feb, 1992).
- 218 19. R. T. Sutton, B. W. Dong, J. M. Gregory, *Geophys Res Lett* **34**, (Jan 16, 2007).

- 219 20. J. D. Annan, J. C. Hargreaves, *Geophys Res Lett* **33**, L06704 (2006).
- 220 21. J. Hansen *et al.*, *The Open Atmospheric Science Journal* **2**, 217 (2008).
- 221 22. D. W. Lea, *J Climate* **17**, 2170 (Jun, 2004).
- 222 23. T. Schneider von Deimling, H. Held, A. Ganopolski, S. Rahmstorf, *Clim Dynam* **27**, 149
223 (Aug, 2006).
- 224 24. A. P. Ballantyne, M. Lavine, T. J. Crowley, J. Liu, P. B. Baker, *Geophys Res Lett* **32**,
225 L05712 (2005).
- 226 25. S. P. Harrison, K. E. Kohfeld, C. Roelandt, T. Claquin, *Earth-Science Reviews* **54**, 43
227 (Jun, 2001).
- 228 26. B. A. Maher *et al.*, *Earth-Science Reviews* **99**, 61 (2010).
- 229 27. M. Crucifix, *Geophys Res Lett* **33**, L18701 (Sep 19, 2006).
- 230 28. A. Schmittner, A. Oschlies, H. D. Matthews, E. D. Galbraith, *Global Biogeochem Cy* **22**,
231 GB1013 (Feb 14, 2008).
- 232 29. S. L. Thompson, S. G. Warren, *J. Atmos. Sci.* **39**, 2667 (1982).
- 233 30. W. R. Peltier, *Annual Review of Planetary Sciences* **32**, 111 (2004).
- 234 31. V. Ramaswamy *et al.*, in *Climate Change 2001: The Scientific Basis. Contribution of*
235 *Working Group I to the Third Assessment Report of the Intergovernmental Panel on*
236 *Climate Change*, J. T. Houghton *et al.*, Eds. (Cambridge University Press, Cambridge,
237 United Kingdom, New York, NY, USA, 2001), pp. 881.
- 238 32. EPICA Community Members, *Nature* **429**, 623 (Jun 10, 2004).
- 239 33. J. Flückiger *et al.*, *Science* **285**, 227 (Jul 9, 1999).
- 240 34. N. M. Mahowald *et al.*, *Geophys Res Lett* **33**, L20705 (2006).
- 241 35. J. Hansen *et al.*, in *Climate Processes and Climate Sensitivity*, J. E. Hansen, T.
242 Takahashi, Eds. (American Geophysical Union, 1984), vol. 29, pp. 130-163.
- 243 36. P. Kohler *et al.*, *Quaternary Sci Rev* **29**, 129 (Jan, 2010).
- 244 37. K. E. Taylor *et al.*, *J Climate* **20**, 2530 (Jun 1, 2007).
- 245 38. A. J. Broccoli, *J Climate* **13**, 951 (Mar 1, 2000).
- 246 39. C. D. Hewitt, J. F. B. Mitchell, *Clim Dynam* **13**, 821 (Nov, 1997).
- 247 40. M. Yoshimori, T. Yokohata, A. Abe-Ouchi, *J Climate* **22**, 3374 (Jun, 2009).
- 248 41. M. Yoshioka *et al.*, *J Climate* **20**, 1445 (Apr 15, 2007).
- 249 42. I. N. Sokolik, O. B. Toon, *Journal of Geophysical Research-Atmospheres* **104**, 9423 (Apr
250 27, 1999).
- 251 43. J. Perlwitz, I. Tegen, R. L. Miller, *Journal of Geophysical Research-Atmospheres* **106**,
252 18167 (Aug 27, 2001).
- 253 44. J. D. Shakun *et al.*, *Nature in review*, (2011).
- 254 45. J. Arbuszewski, P. deMenocal, A. Kaplan, E. C. Farmer, *Earth Planet Sc Lett* **300**, 185
255 (Dec 1, 2010).
- 256 46. E. Mathien-Blard, F. Bassinot, *Geochem Geophys Geosy* **10**, Q12011 (Dec 22, 2009).
- 257 47. O. A. Saenko, A. Schmittner, A. J. Weaver, *J Climate* **17**, 2033 (Jun, 2004).
- 258 48. W. B. Curry, D. W. Oppo, *Paleoceanography* **20**, (Mar 18, 2005).
- 259 49. J. R. Alder, S. W. Hostetler, D. Pollard, A. Schmittner, *Geosci. Model Dev.* **4**, 69 (2011).
- 260 50. M. Jun, M. L. Stein, *Technometrics* **49**, 468 (Nov, 2007).
- 261 51. D. S. Oliver, *Mathematical Geology* **35**, 681 (Aug, 2003).
- 262 52. D. J. Frame *et al.*, *Geophys Res Lett* **32**, L09702 (May 6, 2005).
- 263 53. J. D. Annan, J. C. Hargreaves, *Climatic Change* **104**, 423 (Feb, 2011).

- 264 54. G. O. Roberts, J. S. Rosenthal, *Journal of Computational and Graphical Statistics* **18**,
265 349 (Jun, 2009).
- 266 55. A. Schmittner, T. A. Silva, K. Fraedrich, E. Kirk, F. Lunkeit, *J Climate* **24**, 2814 (2011).
- 267 56. S. P. Harrison, I. C. Prentice, *Global Change Biol* **9**, 983 (Jul, 2003).
- 268 57. R. B. Alley, *Quaternary Sci Rev* **19**, 213 (Jan, 2000).
- 269 58. C. Waelbroeck *et al.*, *Nature* **412**, 724 (Aug 16, 2001).
- 270 59. V. L. Peck, I. R. Hall, R. Zahn, H. Elderfield, *Paleoceanography* **23**, (Sep 24, 2008).
- 271 60. K. Minoshima, H. Kawahata, K. Ikehara, *Palaeogeography Palaeoclimatology*
272 *Palaeoecology* **254**, 430 (Oct 22, 2007).
- 273 61. D. Isono *et al.*, *Geology* **37**, 591 (Jul, 2009).
- 274 62. F. Peterse *et al.*, *Earth Planet Sc Lett* **301**, 256 (Jan 3, 2011).
- 275 63. K. Sawada, N. Handa, *Nature* **392**, 592 (Apr 9, 1998).
- 276 64. A. E. Carlson *et al.*, *Geology* **36**, 991 (Dec, 2008).
- 277 65. I. S. Castaneda *et al.*, *Paleoceanography* **25**, (Mar 10, 2010).
- 278 66. A. Ijiri *et al.*, *Palaeogeography Palaeoclimatology Palaeoecology* **219**, 239 (Apr 18,
279 2005).
- 280 67. M. Ziegler, D. Nurnberg, C. Karas, R. Tiedemann, L. J. Lourens, *Nat Geosci* **1**, 601 (Sep,
281 2008).
- 282 68. H. W. Arz, J. Patzold, P. J. Muller, M. O. Moammar, *Paleoceanography* **18**, (Jun 25,
283 2003).
- 284 69. B. P. Flower, D. W. Hastings, H. W. Hill, T. M. Quinn, *Geology* **32**, 597 (Jul, 2004).
- 285 70. P. deMenocal, J. Ortiz, T. Guilderson, M. Sarnthein, *Science* **288**, 2198 (Jun 23, 2000).
- 286 71. G. J. Wei, W. F. Deng, Y. Liu, X. H. Li, *Palaeogeography Palaeoclimatology*
287 *Palaeoecology* **250**, 126 (Jun 25, 2007).
- 288 72. C. Huguot, J. H. Kim, J. S. S. Damste, S. Schouten, *Paleoceanography* **21**, (Jul 20,
289 2006).
- 290 73. M. W. Schmidt, H. J. Spero, D. W. Lea, *Nature* **428**, 160 (Mar 11, 2004).
- 291 74. G. Leduc *et al.*, *Nature* **445**, 908 (Feb 22, 2007).
- 292 75. H. M. Benway, A. C. Mix, B. A. Haley, G. P. Klinkhammer, *Paleoceanography* **21**,
293 (Aug 16, 2006).
- 294 76. S. Steinke *et al.*, *Quaternary Sci Rev* **27**, 688 (Apr, 2008).
- 295 77. S. Weldeab, D. W. Lea, R. R. Schneider, N. Andersen, *Science* **316**, 1303 (Jun 1, 2007).
- 296 78. S. Weldeab, R. R. Schneider, M. Kolling, G. Wefer, *Geology* **33**, 981 (Dec, 2005).
- 297 79. M. Kienast *et al.*, *Nature* **443**, 846 (Oct 19, 2006).
- 298 80. A. Koutavas, J. P. Sachs, *Paleoceanography* **23**, (Oct 22, 2008).
- 299 81. A. Jaeschke, C. Ruhlemann, H. Arz, G. Heil, G. Lohmann, *Paleoceanography* **22**, (Nov
300 8, 2007).
- 301 82. S. Weldeab, R. R. Schneider, M. Kolling, *Earth Planet Sc Lett* **241**, 699 (Jan 31, 2006).
- 302 83. L. Stott, A. Timmermann, R. Thunell, *Science* **318**, 435 (Oct 19, 2007).
- 303 84. J. W. H. Weijers, E. Schefuss, S. Schouten, J. S. S. Damste, *Science* **315**, 1701 (Mar 23,
304 2007).
- 305 85. E. Schefuss, S. Schouten, R. R. Schneider, *Nature* **437**, 1003 (Oct 13, 2005).
- 306 86. J. E. Tierney *et al.*, *Science* **322**, 252 (Oct 10, 2008).
- 307 87. C. Levi *et al.*, *Geochem Geophys Geosy* **8**, (May 30, 2007).
- 308 88. J. Xu, A. Holbourn, W. G. Kuhnt, Z. M. Jian, H. Kawamura, *Earth Planet Sc Lett* **273**,
309 152 (Aug 30, 2008).

- 310 89. E. C. Farmer, P. B. deMenocal, T. M. Marchitto, *Paleoceanography* **20**, (Jun 29, 2005).
311 90. J. Kaiser, F. Lamy, D. Hebbeln, *Paleoceanography* **20**, (Oct 29, 2005).
312 91. E. Calvo, C. Pelejero, P. De Deckker, G. A. Logan, *Geophys Res Lett* **34**, (Jul 14, 2007).
313 92. K. Pahnke, J. P. Sachs, *Paleoceanography* **21**, (Apr 13, 2006).
314 93. F. Lamy *et al.*, *Earth Planet Sc Lett* **259**, 400 (Jul 30, 2007).
315 94. J. P. Sachs, R. F. Anderson, S. J. Lehman, *Science* **293**, 2077 (Sep 14, 2001).
316 95. S. Barker *et al.*, *Nature* **457**, 1097 (Feb 26, 2009).
317 96. T. T. Barrows, S. J. Lehman, L. K. Fifield, P. De Deckker, *Science* **318**, 86 (Oct 5, 2007).
318 97. B. Stenni *et al.*, *Quaternary Sci Rev* **29**, 146 (Jan, 2010).
319 98. B. Lemieux-Dudon *et al.*, *Quaternary Sci Rev* **29**, 8 (Jan, 2010).
320 99. K. Kawamura *et al.*, *Nature* **448**, 912 (Aug 23, 2007).
321 100. J. R. Petit *et al.*, *Nature* **399**, 429 (Jun 3, 1999).
322 101. E. Kalnay *et al.*, *B Am Meteorol Soc* **77**, 437 (Mar, 1996).
323 102. V. Ramanathan *et al.*, *Science* **243**, 57 (Jan 6, 1989).
324 103. Data are available for download at the National Climatic Data Center at NOAA
325 <http://www.ncdc.noaa.gov> and at
326 <http://mgg.coas.oregonstate.edu/~andreas/data/schmittner11sci>.
327 Acknowledgements: This work was supported by the Paleoclimate Program of the National
328 Science Foundation through project PALEOVAR (06023950-ATM). Thanks to Sandy
329 Harrison and two anonymous reviewers for thoughtful and constructive comments that
330 led to significant improvements of the paper.
331

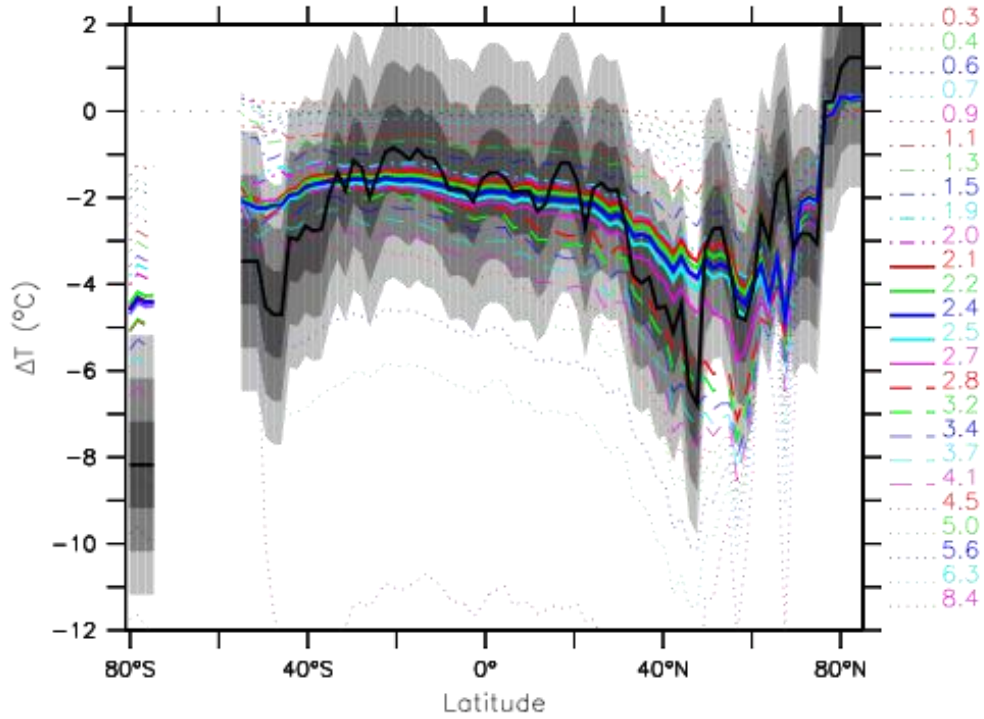
332 **Figures:**



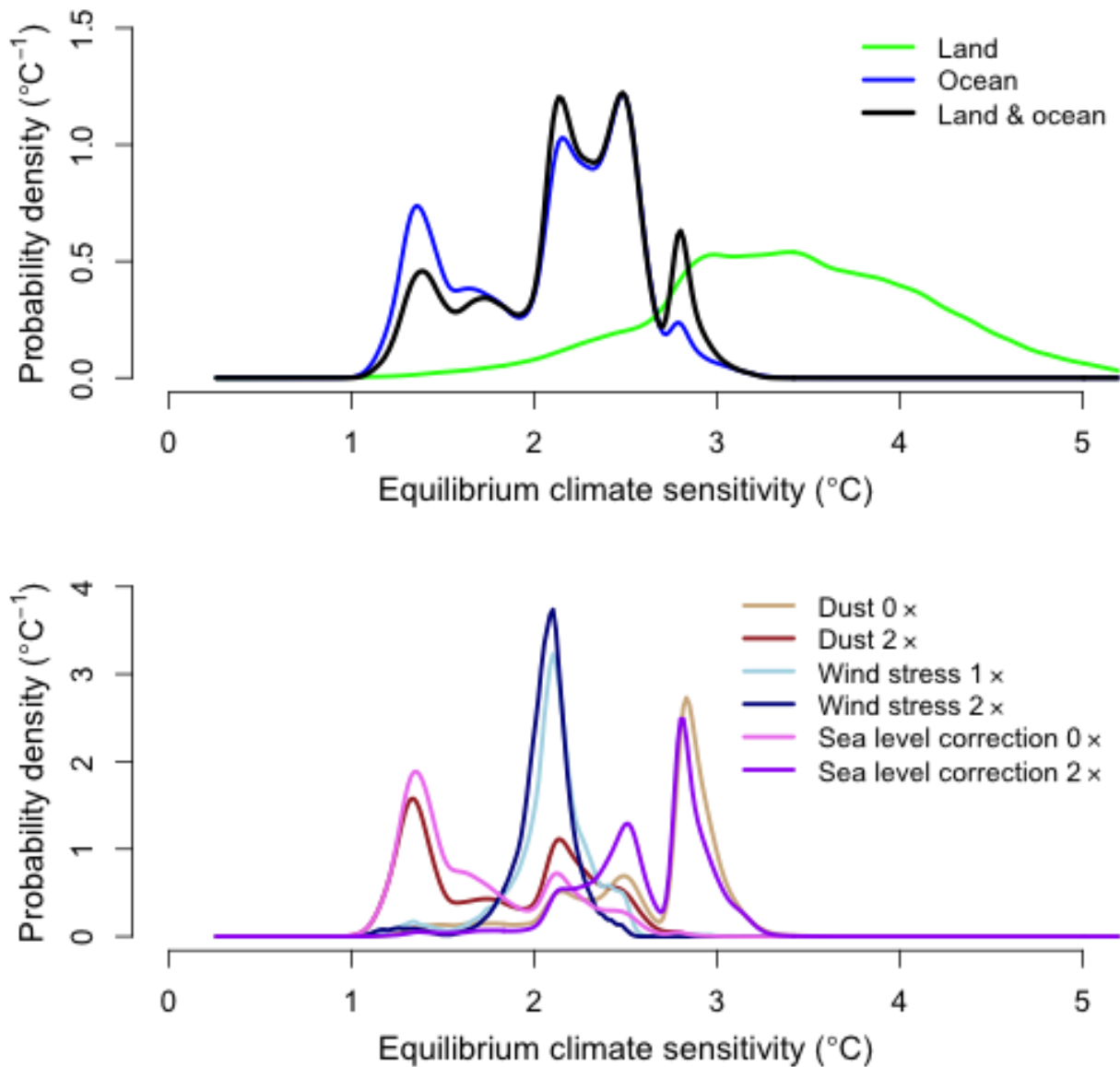
333

334 Figure 1. Annual mean surface temperature (sea surface temperature over oceans and near
335 surface air temperature over land) change between the LGM and modern. Top: Reconstructions
336 of sea surface temperatures from multiple proxies (12), surface air temperatures over land from
337 pollen (13) and additional data (SOM). Bottom: Best-fitting model simulation ($ECS_{2xC} = 2.4 \text{ K}$).

338



339
 340 Figure 2. Zonally averaged surface temperature change between the LGM and modern. The
 341 black thick line denotes the climate reconstructions and grey shading the ± 1 , 2, and 3 K intervals
 342 around the observations. Modeled temperatures, averaged using only cells with reconstructions
 343 (see Fig. 1), are shown as colored lines labeled with the corresponding ECS_{2xC} values.



344

345 Figure 3. Marginal posterior probability distributions for ECS_{2xC} . Upper: estimated from land
 346 and ocean, land only, and ocean only temperature reconstructions using the standard assumptions
 347 ($1 \times$ dust, $0 \times$ wind stress, $1 \times$ sea level correction of $\Delta S_{SL} = 0.32$ K, see SOM). Lower:
 348 estimated under alternate assumptions about dust forcing, wind stress, and ΔS_{SL} using land
 349 and ocean data.